Natural Resources Canada | Ressources naturelles Canada

GEOLOGICAL SURVEY OF CANADA
OPEN FILE 7752

Geometry and regional significance of joint sets in the Ordovician-Silurian Anticosti Basin: new insights from fracture mapping

N. Pinet, V. Brake, and D. Lavoie

2015

Canada

GEOLOGICAL SURVEY OF CANADA
OPEN FILE 7752

Geometry and regional significance of joint sets in the Ordovician-Silurian Anticosti Basin: new insights from fracture mapping

N. Pinet, V. Brake, and D. Lavoie

Geological Survey of Canada, 490, rue de la Couronne, Québec, Quebec

2015

doi:10.4095/295982

This publication is available for free download through GEOSCAN (http://geoscan.nrcan.gc.ca/).

Recommended citation

Pinet. N., Brake, V., and Lavoie, D., 2015. Geometry and regional significance of joint sets in the Ordovician-Silurian Anticosti Basin: new insights from fracture mapping; Geological Survey of Canada, Open File 7752, 25 p. doi:10.4095/295982

Publications in this series have not been edited; they are released as submitted by the author.

Geometry and regional significance of joint sets in the Ordovician-Silurian Anticosti Basin: new insights from fracture mapping

Nicolas Pinet*, Virginia Brake* and Denis Lavoie*

***Natural Resources Canada, Geological Survey of Canada, 490 rue de la Couronne, Quebec, G1K 9A9.

ABSTRACT: Tensile opening-mode fractures (or joints) intensively dissect nearly flat-lying Lower Ordovician to lower Silurian strata in the northern part of the Anticosti Basin. Fracture mapping near Havre-Saint-Pierre, on the Mingan Islands and on Anticosti Island indicates that the two predominant joint sets are nearly orthogonal and trend ~ N100 and ~N10. For the majority of the studied sites, the ~N100 joints are the older and most continuous, suggesting that they form a systematic set of fractures that likely extend to a significant depth. The median spacing of the ~N100 systematic joint set is approximately 1 m and is partly controlled by the mechanical characteristics of the fractured bed. Some joints exhibit significant horizontal and vertical continuity and are locally concentrated in structural corridors, suggesting that they may influence subsurface fluid flow if open at depth. Systematic fractures are interpreted to have formed in a forebulge setting during an episode of local extension.

INTRODUCTION

Subsurface fluid flow is strongly influenced by lithological and structural discontinuities. Secondary permeability originating from fractures may supplement the intrinsic matrix permeability of a rock unit and partly control or even dominate the subsurface fluid-flow pattern. Fracture analysis is thus important to evaluate reservoir rock characteristics and seal rock integrity. Moreover, successful drilling of self-sourced unconventional reservoirs may depend on the presence and characteristics of systematic sets of fractures (Ferrill et al., 2014 and references therein).

In autochthonous domains (or platforms), deformation is often characterized by fracturing (background deformation) with, in some cases, narrow zones of greater deformation (fracture corridors and/or cataclasis along fault zones). This is the case on Anticosti Island, where systematic joint sets intensely dissect the nearly flat-lying sedimentary succession (Bordet et al., 2010).

Our study aims to complement existing data on the background deformation of the northern part of the Anticosti Basin. The study includes a first appraisal of joint patterns at the base of the sedimentary succession, near Havre-Saint-Pierre (Quebec) in order to evaluate the effects of the Taconian and/or Acadian orogenesis. This study is carried out under the GNES (Geoscience for New Energy Supply) program and contributes to a broader investigation of the geomechanical characteristics of the Macasty Formation and overlying strata. It takes place in the context of recent oil shale development and potential exploitation by hydraulic fracturing, with the ultimate goal to gain a better understanding of the seal rocks integrity.

GEOLOGICAL SETTING

The Anticosti Basin is a large sedimentary basin covering the northern part of the Gulf of St. Lawrence (Fig. 1; Sanford, 1993; Mossop et al., 2004). It includes the eastern part of the St. Lawrence Platform, which corresponds to the Paleozoic autochthonous sedimentary cover of the eastern North American craton in Canada and the eastern United States.

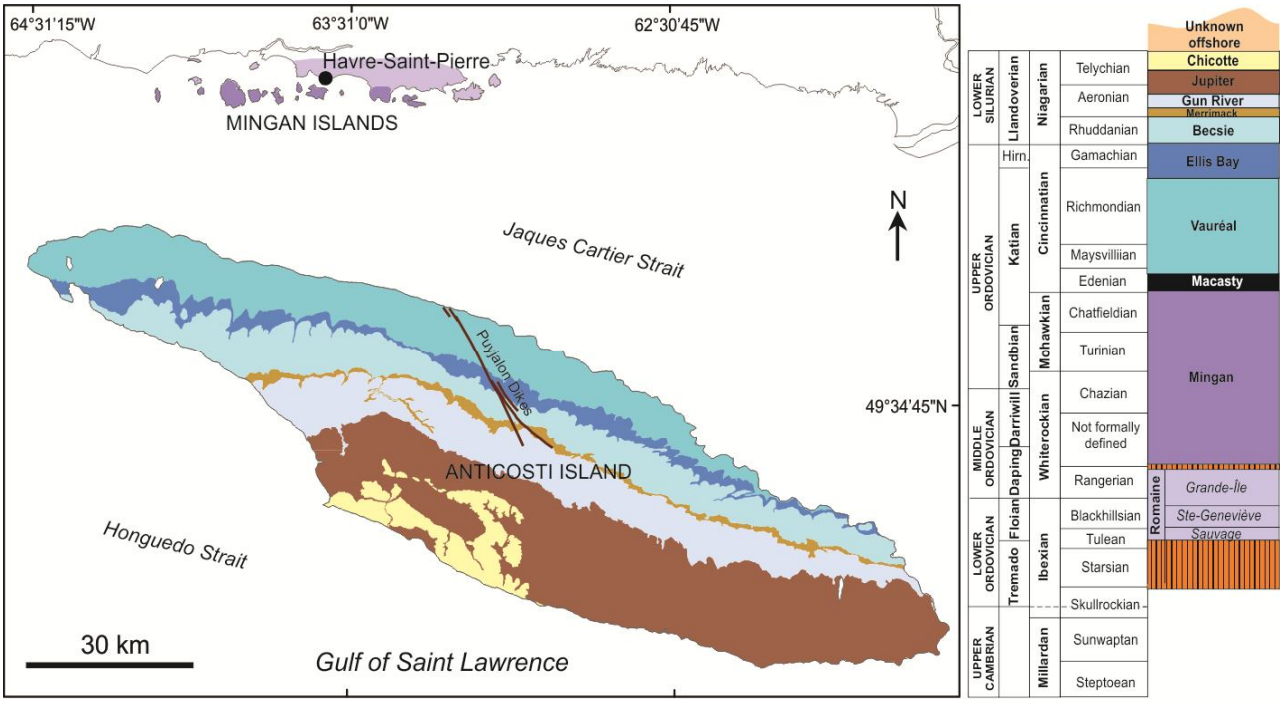

Figure 1: Geological map and stratigraphic column of Anticosti Island and Havre-Saint-Pierre/Mingan islands area. Geology extracted from the Sigeom database (Ministère des Ressources Naturelles du Québec), August 2014.

The onshore succession of the Anticosti-Mingan islands presents several distinct characteristics compared to those of southern Quebec and western Newfoundland (Globensky, 1987; Cooper et al., 2001): 1) it is located farther from the Appalachian structural front and thus less deformed; 2) it recorded a shorter geological history characterized by the lack of Cambrian to earliest Ordovician strata (Sanford, 1993) and, 3) it is far more stratigraphically continuous and lacks major tectonic-related sedimentary hiatus (Long, 2007).

In the northern part of the Anticosti Basin, the sedimentary beds dip gently (approximately 3°) toward the southwest (SOQUIP, 1987). The base of the succession is exposed near Havre-Saint-Pierre and unconformably overlies the metamorphic rocks of the Canadian Shield (Grenville Province). Basal strata correspond to a 400-800 m thick passive margin peritidal-dominated, limestone and dolostone assemblage (Lower Ordovician Romaine Formation; Desrochers and James, 1988; Desrochers et al., 2012). Along the north shore of the Gulf of St. Lawrence and on the

Mingan islands, this assemblage is unconformably overlain by a 400-600 m thick Taconian shallow marine foreland basin succession in which basal siliciclastics were succeeded by predominantly open marine carbonates (Middle Ordovician Mingan Formation; Desrochers, 1988). The overlying Upper Ordovician Macasty Formation forms part of the seafloor bedrock between Mingan and Anticosti islands, but it is not exposed onshore. It corresponds to a 25-175 m thick interval of dark marine limy shale documented in wells that is presently the main focus of unconventional hydrocarbon exploration in the area. Overlying units are exposed on Anticosti Island and include: 1) a 900-1200 m thick siltstone-dominated interval overlain by outer ramp shallowing-upward carbonates (Vauréal Formation); 2) subtidal carbonates with local bioherms (Ellis Bay Formation; ~ 60 m thick); 3) various carbonate facies with minor siliciclastics deposited on a storm-dominated carbonate ramp (~400 thick Anticosti Group; Sami and Desrochers, 1992; Desrochers, 2006). Offshore, south of Anticosti Island, approximately 1140 m of younger sedimentary units complete the Anticosti Basin succession (Pinet et al., 2012).

On Anticosti/Mingan islands, the exposed sedimentary succession is weakly deformed, affected by only minor structural features (fractures, minor faults) that record the distant foreland strain associated with Appalachian orogenesis and younger events (Bordet et al., 2010). Seismic interpretation on Anticosti Island indicates that the base of the sedimentary succession is affected by steeply-dipping normal faults (including the Jupiter Fault) that do not extend into the Silurian units (Lynch, 2000; Castonguay et al., 2005; Bordet et al., 2010). South of Anticosti Island, the offshore part of the basin includes a 40 km wide fold-and-fault belt oriented sub-parallel to the coastline of the Gaspé Peninsula. The structural style of the offshore domain is characterized by broad open synclines, narrow anticlines and NW-striking faults with dextral strike separations (Pinet et al., 2012).

METHODOLOGY

In this paper, the term fracture is used as a general term describing any discontinuity within a rock mass that developed in response to stress, whereas the term joint is restricted to fractures displaying no visible in-plane displacement (Bonnet et al., 2001),

Three main methods were used to characterize the background deformation and joint characteristics (Table 1): 1) sampling the traces that intersect a line drawn on the exposure, either the pavement or vertical wall (scanline sampling); 2) sampling the traces that intersect a circle drawn on the pavement (circle sampling) and 3) sampling the traces within a finite size area on the pavement (area sampling). The choice of a specific method was mainly guided by the types of exposures.

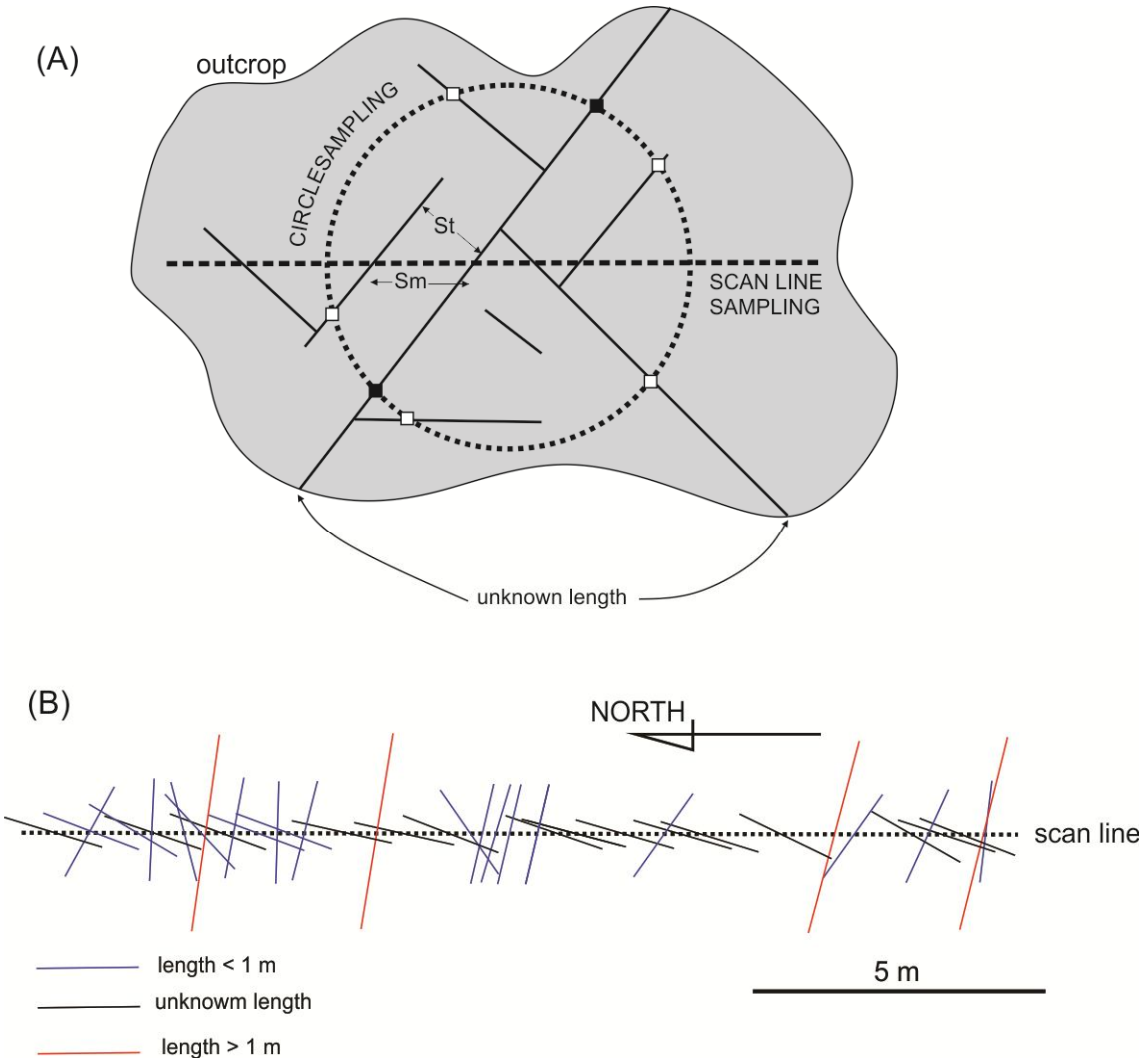

Figure 2: (A) Sketch illustrating the scanline and circle sampling methods. For the scanline sampling method, a trigonometric correction is necessary because the measured spacing (Sm) between two joint of the same set is not the true spacing (St). For the circular sampling, the total number of joint crossing the circle are counted (white and black squares), as well the number of joint crossing the entire circle (black square). (B) Example of joint distribution along a scanline (site: Anticosti 1).

During scanline sampling, the joint spacing, strike, dip, length and crosscutting/abutting relationships with other structural elements have been measured. Joint length refers to the horizontal extension of the joint on pavements and to its vertical extension for outcrop walls. In both cases, length measurements suffer a censoring bias as long joints may extend beyond the bedrock exposure and thus represent minimum lengths. In other words, the length of the longer joints, which are most efficient in ensuring fractures connectivity, is poorly constrained in most cases. Fracture aperture and fill were proven difficult to characterize quantitatively due to meteoritic weathering and will not be discussed in this paper.

Scanline sampling is subject to an orientation bias that depends on the relative orientation between the scanline

and the discontinuity (Fig. 2). This bias can be mitigated by applying a trigonometric correction taking into account the acute angle between a specific joint set and the scanline, in order to determine the 'true' spacing of structures (Terzaghi, 1965). In cases where joint sets formed a rectangular grid, the measurements along two perpendicular scanlines have accurately described the joint pattern, without the need of an additional correction.

Fracture density (D), defined by the number of fractures per meter, is

$D = N/L$

Where N is the number of fractures and L the length of the scanline.

Fracture spacing (S), defined as the average distance between two fractures, is:

$S = 1/D$

The aim of circular scanline sampling is to provide a rapid non-biased estimate of the fracture density (Fig. 2) where the only parameters noted were the number of fractures intersecting the circle (Nm) and the number of fracture crosscutting the entire circle (Nc). The number of fracture (N) is:

$N = Nm - \frac{1}{2} Nc$

Fracture density is

$D = N/2\pi r$

Where r, is the radius of the circle.

GENERAL FRACTURE CHARACTERISTICS

Fracture type

Most of fractures observed in the field are steeply-dipping (> 80°) to vertical tensile opening-mode fractures (or joints) with little or no displacement parallel to the fracture plane. Direct indicators of displacement such as slickenlines were only noted on three fracture planes out of more than 900 measurements. These three slickensided fractures occurred in the Romaine Formation, at the base of the sedimentary succession, on which shallowly-plunging slickenlines indicate predominant left-lateral strike-slip motion (Table 2). The timing of displacement remains unknown and it is therefore not clear if the fractures originally formed as shear fractures or if tensile opening-mode fractures were reactivated after their formation.

Joint set geometry

On pavements, three types of joint patterns can be qualitatively distinguished.

- Pattern I in which two orthogonal sets of relatively long (generally > 1 m; often > 5 m) and linear joint represent more than 80% of the entire joint population (Fig. 3 and 4A).
- Pattern II in which a significant number of joints (>20%) differ in strike from the orthogonal joint sets (Fig. 4C and D)
- Pattern III which is characterized by often curvilinear joints of various orientations (Fig. 4B).

On outcrop walls, these three types of joint pattern can also be recognized, but the crosscutting relationship between joint sets is less obvious.

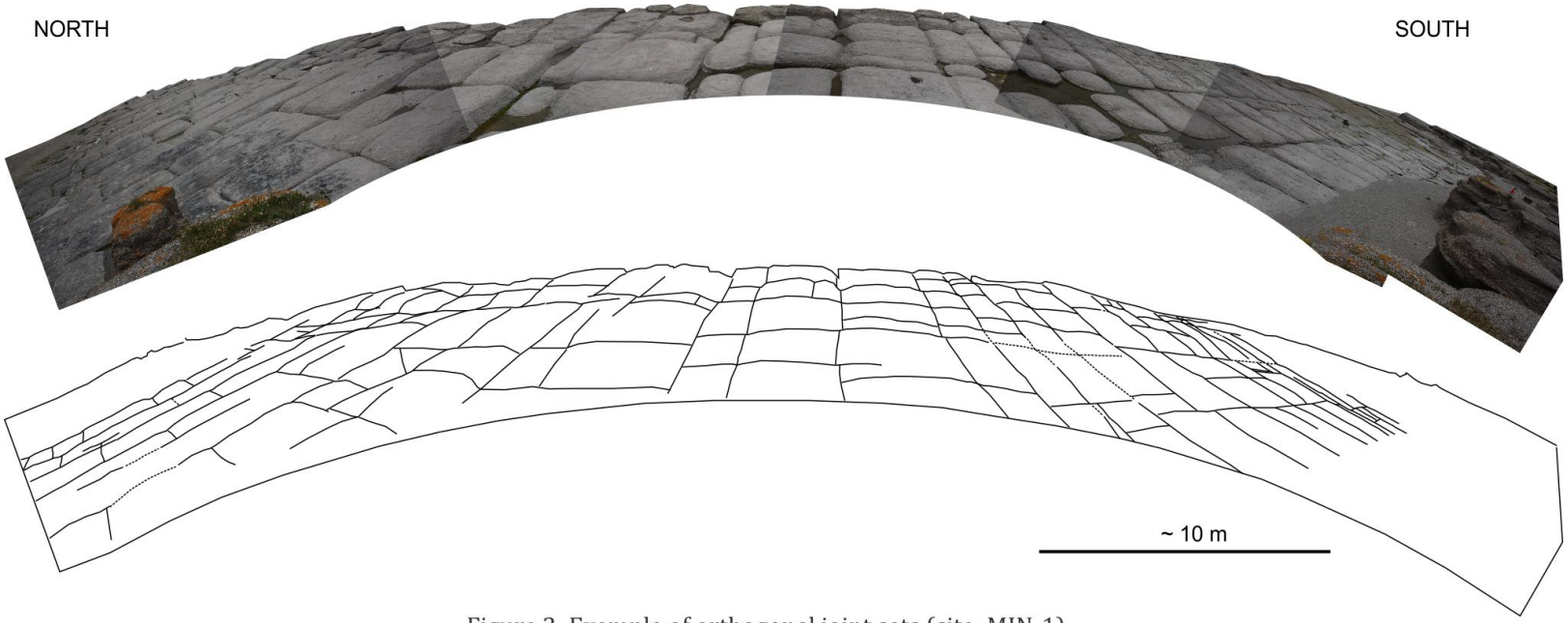

Figure 3: Example of orthogonal joint sets (site: MIN-1).

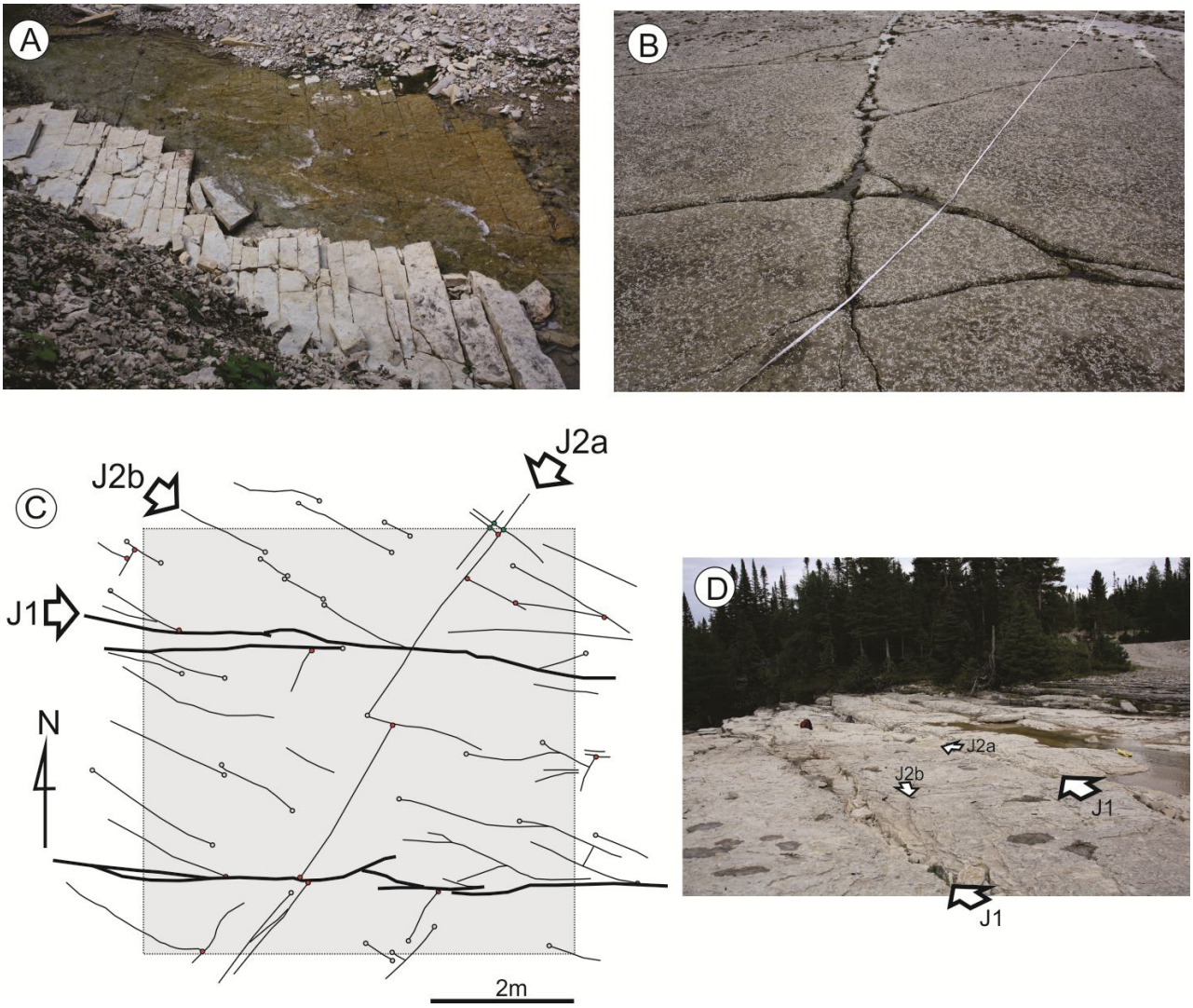

Figure 4: Variation in the joint pattern on horizontal surfaces (pavements). (A) Orthogonal joint pattern (I) characterized by undeformed blocks with a length to width ratio of ~3 or more (site: ANT-13). (B) Irregular joint pattern (III); site: MIN-11. (C) and (D) map and photo of joint pattern II in which the systematic fractures of set J1 are longer but fewer than that of the other sets (J2a and J2b; site: ANT-19).

Crosscutting relationships

On pavements, a specific joint may abut against another joint, or cut it, this latter being continuous on both sides of the joint or not (Fig. 5A and B). In general, in areas characterized by an orthogonal joint pattern, the shorter joint set abuts against the longer one, although the contrary relationship may be observed on the same outcrop. Sub-parallel joints may also display one or both endpoints that are not connected to another fracture (Fig. 5C). In this case, two parallel *en echelon* fractures often present centimetric to decimetric overlapping zones (Fig. 5C). In most cases, these overlapping *en echelon* fractures are nearly straight implying the influence of a remote non-isotropic field stress characterized by a significant differential stress (Olson and Pollard, 1989).

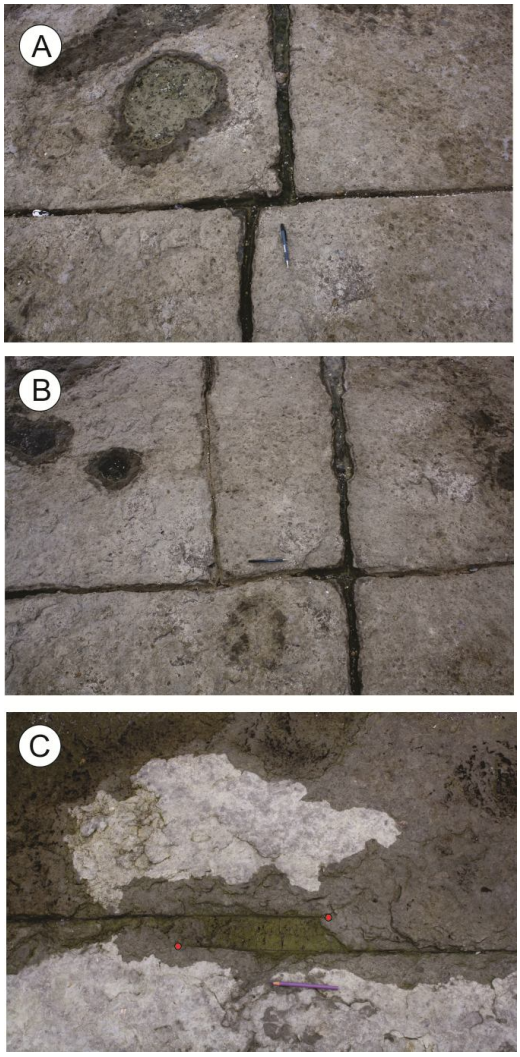

Figure 5: Crosscutting and abutting relationships between fracture sets. (A) Abutting relationship (site: MIN-04); (B) both abutting and crossing relationships (site: MIN-04); (C) en echelon fractures. Red points indicate fracture terminations (site: MIN-02).

Among studied pavements for which fracture terminations have been noted, 16 % present two end-points with no abutting or cutting relationship; 19 % one end-point and one abutting or cutting relationship and 65 % exhibit two or more connections with other fractures. These estimations represent a semi-quantitative evaluation of the connectivity of the fracture system.

The *en echelon* distribution of short, locally pseudo sigmoidal, fractures (<1m) arranged along an obliquely-trending corridor has been noted at two localities (Fig. 6 A to C); these are interpreted as evidence of limited strike-slip shear parallel to the fracture corridor.

Main joint set orientation

Two orientations of joint sets dominate in the study area: ~N100 and ~N10 (Fig. 7 and Table 2). In some cases, the two sets exhibit similar joint density, whereas in other cases, one set is dominant.

The main sets often differ by the length of their joints and their crosscutting relationships. In many cases is it possible to define a set of longer joints (systematic joints) and a second set mainly perpendicular to, and abutting against the first set (cross-joints). Among the 28 sites studied, 20 were interpreted as exhibiting a systematic joint set trending ~N100 (13 on Anticosti Island; 7 in the Havre-Saint-Pierre/Mingan area), 3 a systematic joint set trending ~N10 (1 on Anticosti Island; 2 in the Havre-Saint-Pierre/Mingan area), and 5 were judged ambiguous (2 on Anticosti Island; 3 in the Havre-Saint-Pierre/Mingan area).

These observations indicate that the ~N100 set is predominant, occurs regionally, and probably represents the only set that should be interpreted as an indicator of the paleo-stress field.

Fracture density and spacing

Measured fracture density among the studied sites varies significantly from less than 0.2 fracture/meter to more than 4 fractures/meter (Table 2). After a trigonometric correction to take the scanline orientation into account, the range of fracture density is even wider (0.2 to 9.5 fractures/meter; Table 2). However, comparison of fracture density measurements from different locations should be done with caution, unless results are normalized to a common range of fracture sizes (lengths). Moreover, vertical walls generally exhibit more fractures than

pavement, introducing a bias in the comparison.

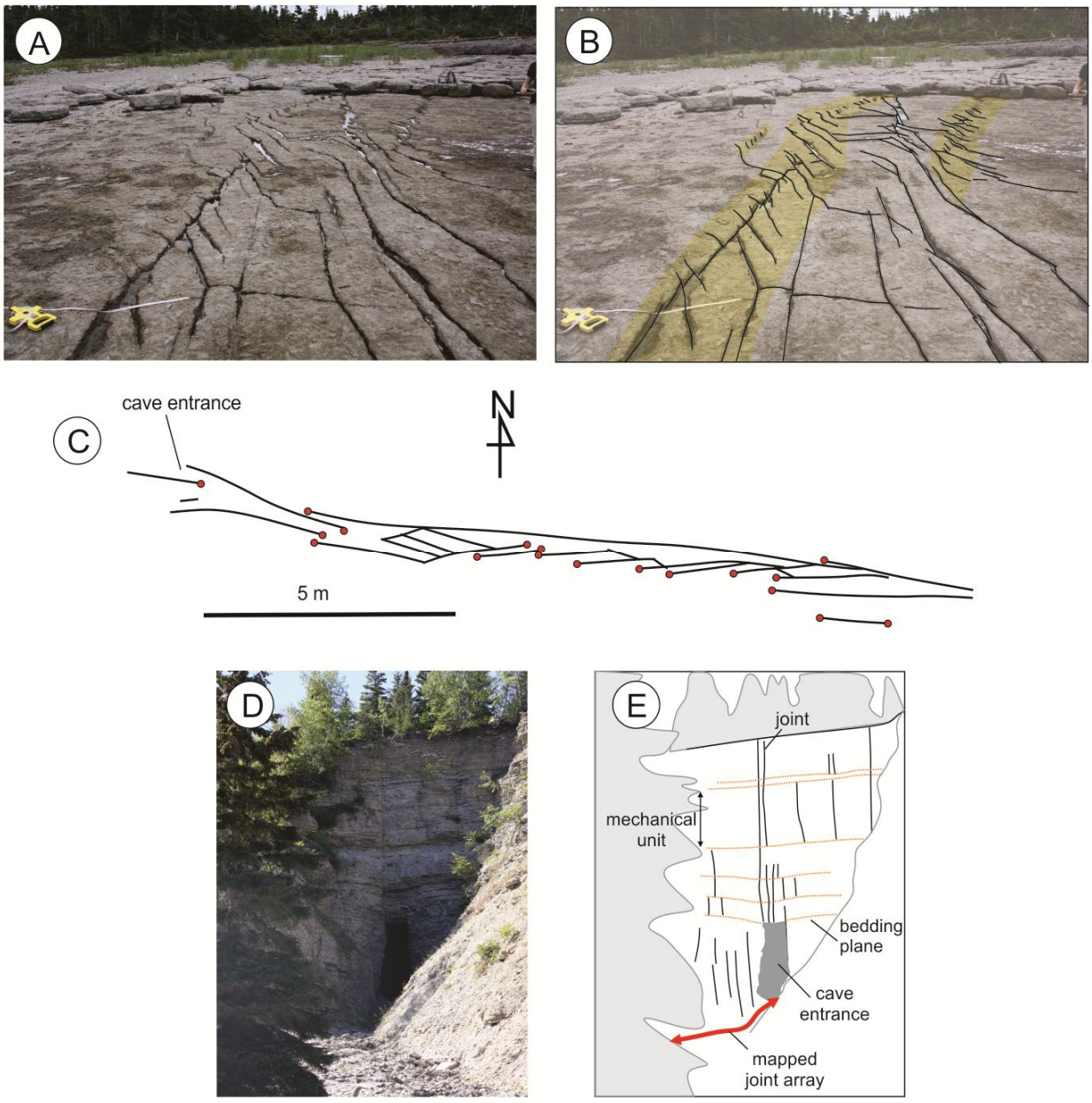

Figure 6: En echelon fractures implying probable motion parallel to the fracture wall. (A) and (B) site: MIN-03. Yellow zones represent structural corridors characterized by obliquely trending en echelon fractures; (C) map, (D), photo, and (E) sketch of photo of site: ANT-18 (grotte de la Patate). Red points in (C) indicate fracture terminations. Note that the orientation of the cave (Figs C and D) is controlled by a ~N100 trending fracture corridor.

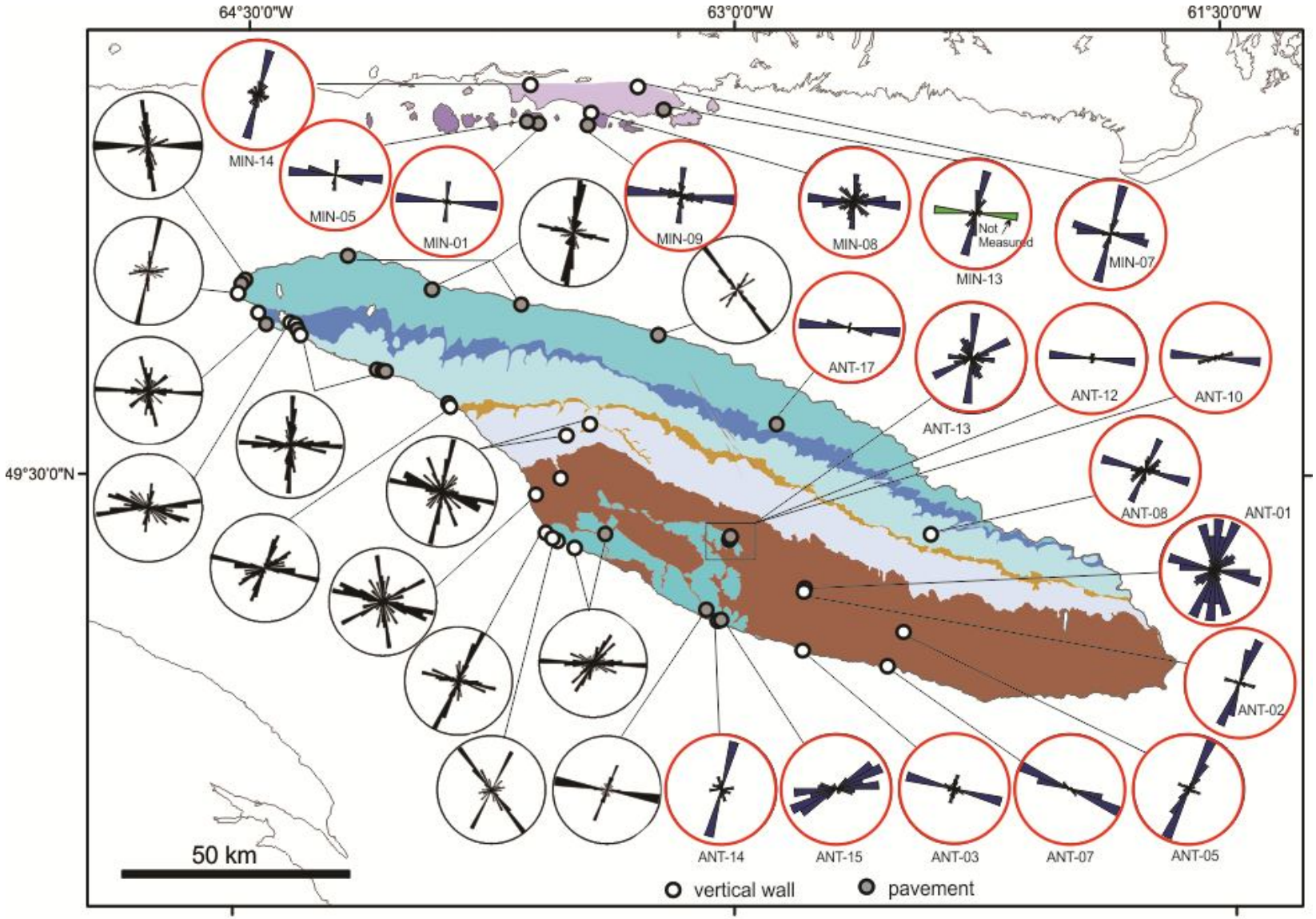

Figure 7: Rose diagrams showing the distribution of fractures near Havre-Saint-Pierre and on Anticosti and Mingan islands. Rose diagram in the eastern part of Anticosti Island (red outline) are from this study. Others are from Bordet et al. (2010).

As noted in numerous fracture studies (e.g. Narr and Suppe, 1991), fracture density displays an approximately linear relationship with bed thickness: the thicker beds are less fractured than thinner ones. However, a quantitative analysis of such relationship was impossible due to the relatively small thickness variation of beds at studied sites.

A parameter that is less influenced by short, randomly oriented fractures, is the spacing of the main join set that ranges from 0.2 to 3.2 m with an median value around 1 m (average = 1.2 m, Fig. 8 and Table 2) for both the Havre-Saint-Pierre/Mingan and Anticosti areas. This value also applies to the sites characterized by an orthogonal joint pattern for which a scanline was oriented perpendicular to the main set. At those sites, the maximal length of the non-fractured block varies between 4.2 and 14.8 m.

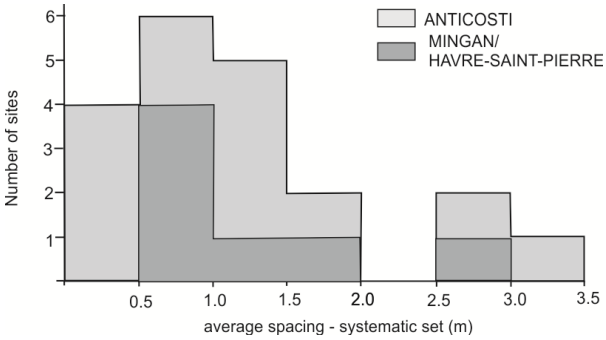

Figure 8: Histogram of the average spacing of the systematic set.

The spacing of the main joint set provides information on the background deformation. However, relatively narrow (< 5 m) zones of more intense fracturing have been documented (Fig. 9). These fracture corridors are generally characterized by subparallel joints including some with greater than average vertical extent. In some cases, fracture corridors have a clear geomorphological signature (Fig. 9A and B).

Fracture length

On pavements, fractures are frequently several meters long and those exceeding the size of the outcrop are common (Fig. 10).

On vertical walls, joints tend to be largely confined within individual beds, leading to the development of 'stratabound' joint systems (Fig. 11). This geometry is enhanced when lithological contacts coincide with mechanical contrasts and act as barriers to fracture propagation. However, in most studied outcrops, a few fractures cut the entire wall and are thus characterized by a significant vertical extent, well above the thickness of single beds.

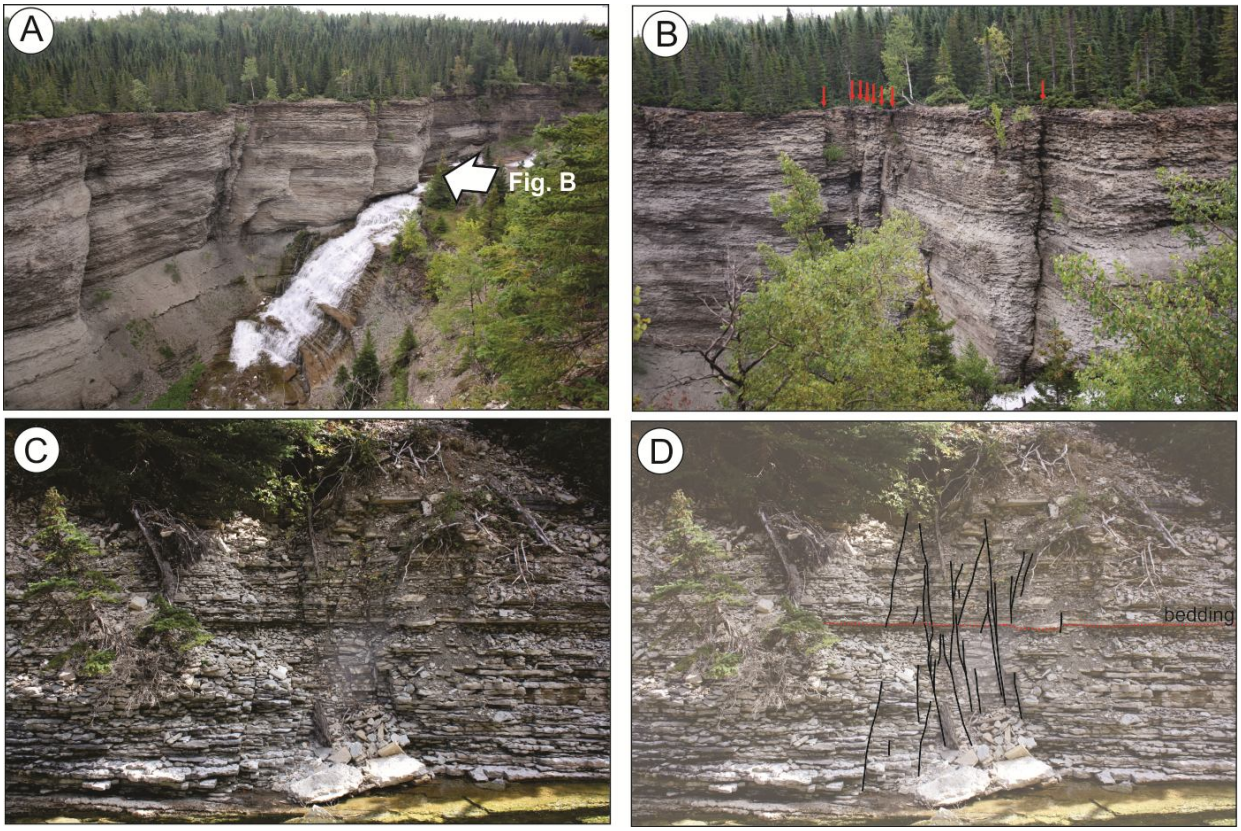

Figure 9: Fracture corridors. (A) and (B) canyon de l'Observation. Note that the waterfall is controlled by a set of narrow spaced fractures (red arrows in B). (C) and (D): site ANT-12.

Figure 10: Example of a very continuous (>25 m) and linear fracture. Note that the fracture does not cut the overlying bed (dark patch in the central part of the photo). Near site MIN-11.

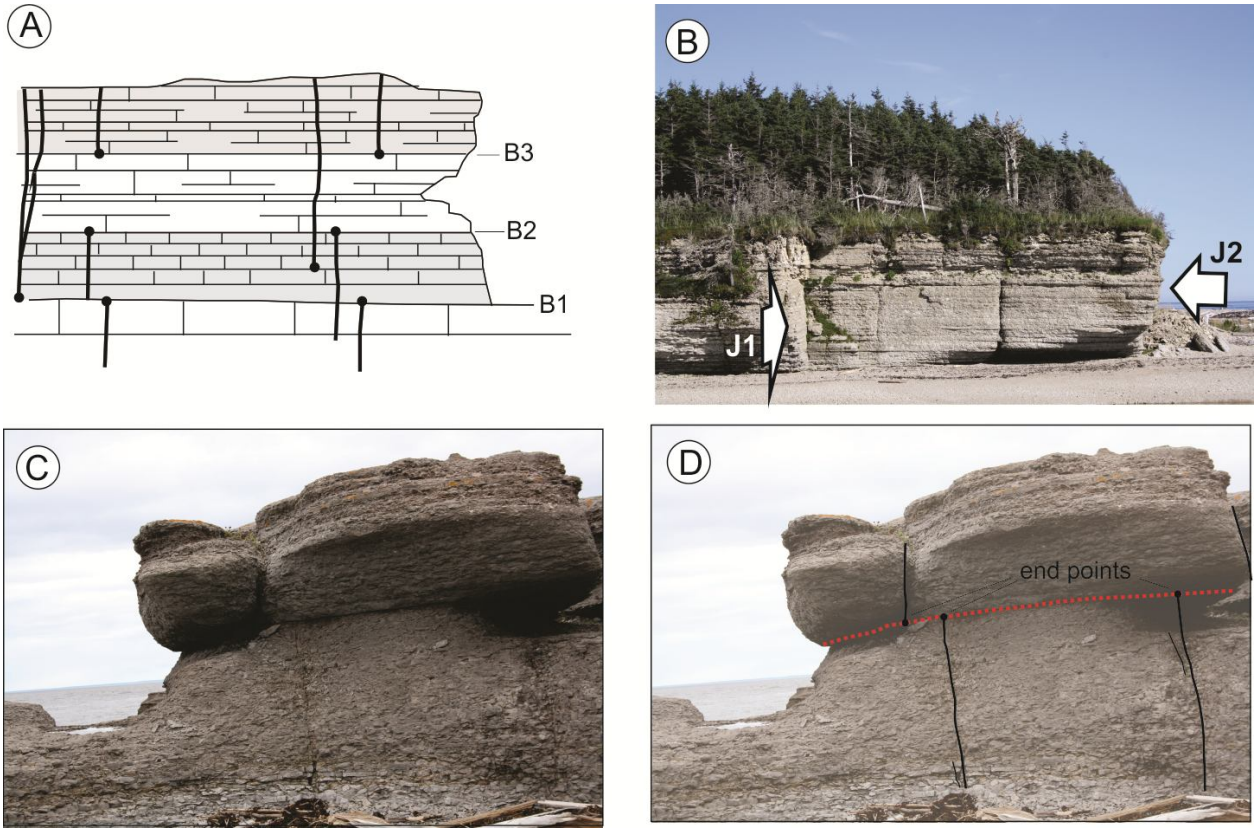

Figure 11: Vertical extent of joints. (A) Sketch showing that some bedding interfaces (B1, B2 and B3) act as structural barriers and control most of joint terminations (drawn from site ANT-03). (B) Example of orthogonal joint sets cutting the entire vertical wall (site ANT-03). (C) and (D) example of stratabound joints; site MIN-01.

DISCUSSION

Interpretation of orthogonal joint pattern

Joint patterns characterized by two orthogonal sets perpendicular to bedding are recognized in many areas and are generally of regional extent (Rives et al., 1994, Caputo, 1995). Joints of the systematic set are longer, more planar and have a clear influence on the formation of cross-joints. However, the exact mechanisms leading to cross-joint formation is still under debate and several interpretations have been proposed including:

1) A stress change due to the development of the first set without regional stress rotation, in particular in the case of narrowly spaced systematic joints (Bai et al., 2002).

2) The warping of joint-bounded rock strip that may induce a local tensile stress field (Granier and Bles, 1988).

3) A stress drop that may be sufficient to reverse the direction of the two sub-horizontal medium ($\sigma 2$) and minimum stresses ($\sigma 3$) if they are of nearly similar magnitude (Hancock et al., 1987).

4) A visco-elastic post-tectonic relaxation effect (Nickelsen and Hough, 1967) during unloading (uplift) that allow rock layers to recover their initial geometry (Rives et al, 1994).

The hypothesis of separate stress events leading to orthogonal joint set formation seems in most cases unrealistic as orthogonal joint sets have been described in Quaternary deposits in areas with no significant regional stress change (Caputo, 1995)

The implication of the mechanical interpretation of orthogonal joint sets is important and should be considered paramount. In interpretations 1 and 3, the formation of the systematic set of joints induces stresses that cause the simultaneous formation of a complimentary, orthogonal set. In these scenarios, both sets form at the same time and are thus expected to be present down to the same depth. Inversely, cross-joints in interpretation 4 (and possibly 2) may form relatively late and may be present only at shallow depth.

In the study area, the regularity of the orthogonal pattern characterized by relatively long (generally > 1 m on pavements), planar cross-joints that in some cases cut the systematic joint set strongly suggest that both sets formed under the same stress field and extent at similar depths.

Influence of sedimentary facies

In relatively undeformed sedimentary rocks, both distribution and spacing of joints are typically controlled by stratigraphy (mechanical thickness and lithological characteristics). The relationship between mechanical thickness, a parameter often correlated to bed thickness, and joint spacing has been demonstrated for decades.

Moreover, for a given thickness of individual mechanical units, high content in calcite (i.e, low content in terrigeneous quartz-rich material), low amount of clay minerals, finer grain size and low values of porosity are commonly associated with stiffer carbonates and, hence, denser bed-perpendicular joint sets (Rustichelli et al., 2013).

Our observations indicate that the joint pattern varies significantly despite little variation in bed thicknesses. This variability is qualitatively attributed to the lithological characteristics of strata and, in particular, to bedding plane characteristics. Strata with a clear lithological variation compared with surrounding beds and planar bedding surfaces tend to have well organized joint patterns, whereas strata with non-planar bedding surfaces tend to have a more irregular geometry (Fig. 12). This relationship is well illustrated on a geomorphologic map of the Mingan archipelago (Environnement Canada, 1991) that show areas characterized by a regular orthogonal pattern ('site rocheux en damier'). These areas are restricted to the southern part of the archipelago, and to an interval of the Mingan Formation.

Spacing of the main set and the concept of fracture saturation

Field studies in other geological settings worldwide indicate that the fracture spacing to layer thickness ratio commonly varies between 0.8 and 1.2. Theoretical modelling (Bai and Pollard, 2000) corroborates such observations as the stress regime changes when the fracture spacing to layer thickness ratio reaches a critical value. Both field-based observations and modeling suggest that a fracture saturation level exists and that a maximum fracture density may be reached.

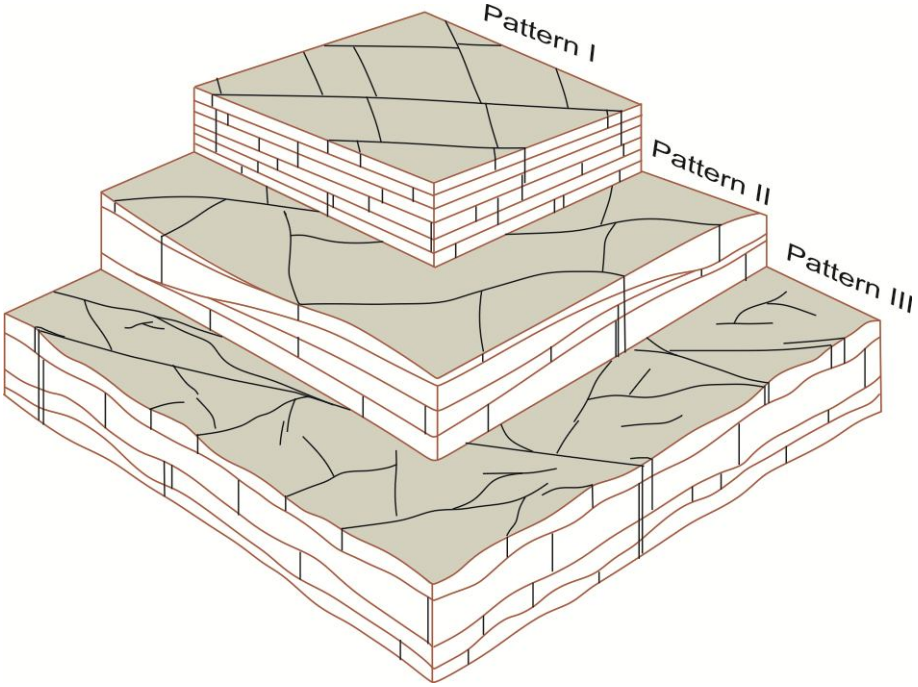

Figure 12: Sketch illustrating the influence of lithology on the joint pattern. Note that pattern I is developed in well bedded intervals, whereas fracture pattern III is preferentially developed in intervals characterized by irregular bedding.

In the study area, the fracture spacing to thickness ratio is greater than 1.2, an indication that the jointing process has not reached the saturation level.

Fracture corridor above the Jupiter Fault

Three geological sections (sites ANT01-02, ANT05 and ANT10-13, Figure 7) were selected to test if the upward extension of the Jupiter Fault, which affects Ordovician strata in the subsurface, is also characterized by fracture corridors in overlying Silurian strata. Unfortunately, none of the sections above the Jupiter Fault had enough bedrock exposures to qualitatively or quantitatively document a variation in fracturing intensity. Considering that these sections were the most promising, field data will probably not provide evidence for testing the hypothesis of the presence of fracture corridors above basement faults.

Tectonic interpretation of the main joint sets

Joints are sensitive tectonic indicators that can be used to infer the orientation of the regional stress field during their development, and in some cases its evolution.

Joints form when the effective tensile stress reaches the tensile strength, which is commonly one order of magnitude less than the shear strength required for faulting. For this reason, opening-mode fractures can form readily under many different conditions corresponding to various stress regimes.

Regional fracture mapping in foreland and platform settings have documented consistent joint patterns that are interpreted as formed either via fluid overpressure in compressional settings or via direct extension (Fig. 13). Formation mechanisms may be distinguished on the basis of geometrical relationships with other structural elements: 1) joint sets

formed via fluid overpressure in compressional settings tend to be characterized by a systematic joint set trending perpendicular to fold axes in the adjacent fold and thrust belt (Engelder, 1985); 2) joints sets formed via direct extension are interpreted to be linked with the tensile flexural stresses contemporaneous with mountains building in adjacent orogenic areas. These are characterized by systematic joints trending parallel to the deformation front (Billi and Salvini; 2003; Billi et al. 2006; Lash and Engelder, 2007).

In the study area, the ~N100 systematic joint set is approximately parallel with the deformation front documented south of Anticosti Island (Pinet et al., 2012), suggesting that it formed through extension, at the extrados of a lithospheric scale forebulge. Consequently, these systematic joints would be contemporaneous with the Middle-Late Devonian Acadian orogeny that caused significant crustal thickening in the northern Appalachians.

The Ordovician part of the Anticosti Basin sedimentary succession is partly contemporaneous with the Taconian orogeny, but the far-field effects of this deformation event are unclear.

Comparison of synthesis rose diagrams for Ordovician (Havre-Saint-Pierre/ Mingan) and Silurian (Anticosti Island) strata shows that predominant fracture sets exhibit similar trends (Fig. 14). However, the relative number of systematic fractures is greater on Anticosti Island compared to the Havre-Saint-Pierre/Mingan area. The significance of this observation is unclear because results have not been normalized to a common fracture size (length). The effects of lithological changes (bed thickness and calcite/dolomite content) in both areas and of Ordovician jointing remain to be investigated in more details.

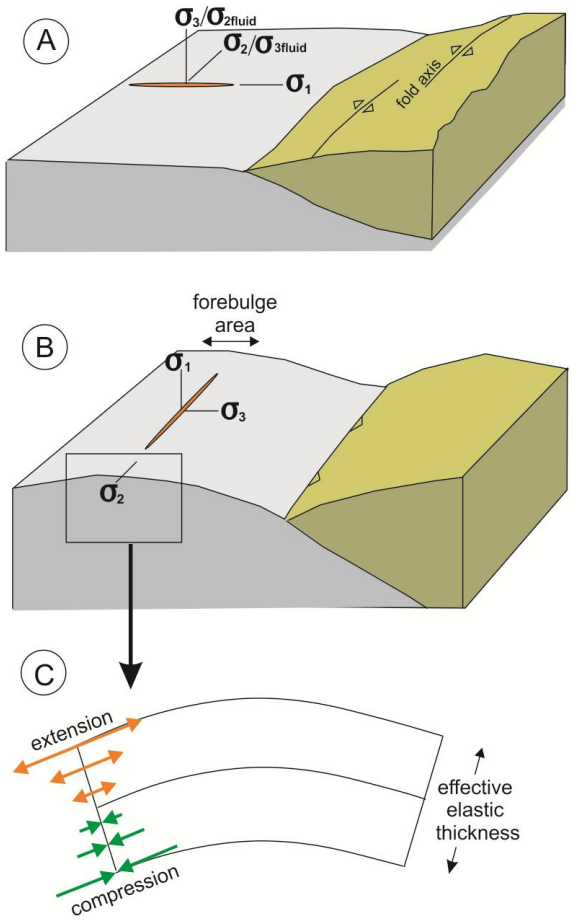

Figure 13: Tectonic setting of joints in foreland and platform areas. (A) Joints formed via fluid overpressure tend to be characterized by a systematic joint set trending perpendicular to fold axes in the adjacent fold and thrust belt; (B) joints formed via direct extension are interpreted to be linked with the tensile flexure-related stresses in a forebulge setting. (A) and (B) are not at the same scale. (C) Variation of the amount of extension with depth in the forebulge area.

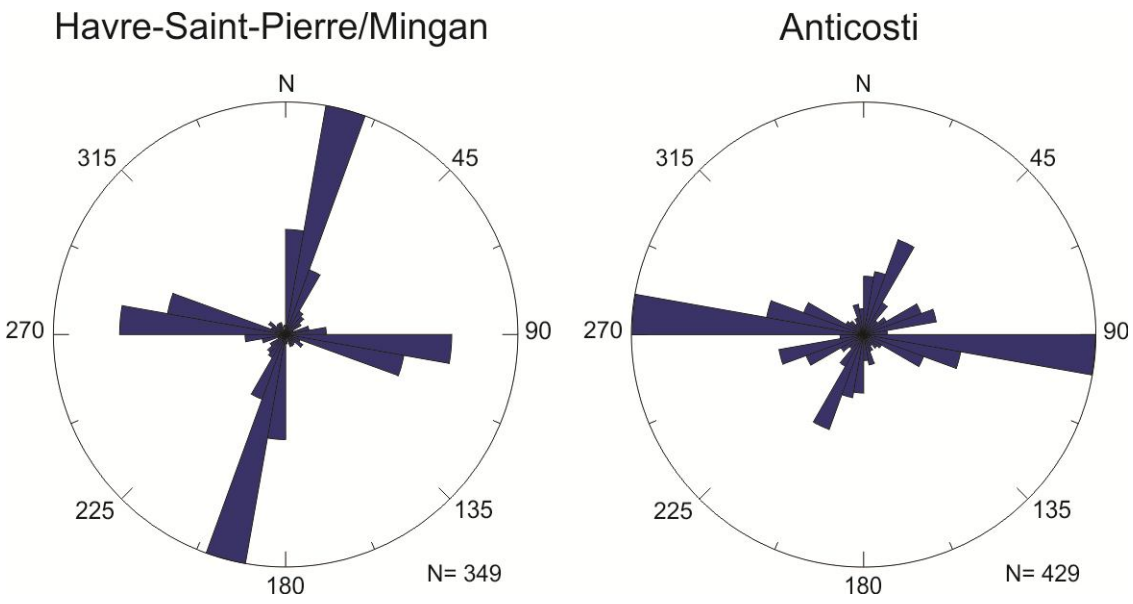

Figure 14: Synthesis rose-diagrams for Ordovician strata (Havre-Saint-Pierre/Mingan area) and Silurian strata (Anticosti Island).

Persistence of fracture sets at depth

In some settings, fractures observed at surface may provide information on fractures present at depth. From a mechanical point of view, it is important to distinguish joint sets formed at depth prior to uplift in response to abnormal fluid pressures or direct extension (tectonic and hydraulic joints of Engelder, 1985) from joint sets formed near the surface in response to thermal-elastic contraction accompanying erosion and uplift (unloading and release joints of Engelder, 1985). This distinction also has practical applications as only the regional joint sets formed prior to uplift are expected to be present in the still deeply (> km) buried sedimentary succession.

Three criteria are qualitatively used to infer the persistence of joints at depth: 1) *age*: older structures generally formed during burial or close to maximal burial conditions dismissing a genetic relationship with exhumation; 2) *geometry*: planar joint are expected to have formed at relatively high stress levels; 3) *orientation*: joints formed due to remote (tectonic) stress field exhibit constant regional scale orientations.

In the northern part of the Anticosti Basin, only the ~N100 and ~N10 joint sets respect all of the above criteria suggesting that they likely extend at depth. This observation suggest that: 1) the extrapolation of other joint sets observed at the surface to depth may overestimate fracture density; 2) joint spacing of the main set is probably the single most useful parameter to characterize jointing , even if it is expected to vary with bed mechanical properties.

Numerical modelling of the Sicilian forebulge (Billi et al., 2006) shows that joint formation linked to plate flexure may occur to depths on the order of 3-5 km. However, joint spacing is expected to decrease slightly with depth as the amount of extension is maximal near the surface (Fig. 13C).

Influence of fractures on subsurface fluid flow

The influence of joints on subsurface fluid flow mainly depends upon their hydraulic properties that are mainly related to their aperture, a parameter that is widely viewed as partly controlled by the current stress regime. Fractures aligned parallel to the present-day maximum principal stress tend to be open whereas fractures perpendicular to it generally present no significant aperture.

In the Gulf of St. Lawrence and adjacent areas, the maximum horizontal compressional stress regionally trends ENE (Reiter et al., 2014), oblique to both the ~N100 and ~N10 joint sets. However, without more detailed additional evidence from wells, the aperture of fracture at depth remains poorly constrained.

CONCLUSION

Fracture mapping near Havre-Saint-Pierre, on the Mingan archipelago and on Anticosti Island has documented consistent regionally-developed joint patterns in nearly flat-lying Lower Ordovician to lower Silurian strata, indicating that their development was mainly controlled by the principal stress trajectories. The predominant, nearly orthogonal, ~ N100 and ~ N10 fracture sets probably formed in a forebulge setting during an episode of local extension.

These observations may be useful to predict the fracture pattern at depth and its influence on subsurface fluid flow. However, more information is needed on the aperture of joints and on the characteristics of fractures in shale-dominated lithologies, two parameters that may be important to characterize the seal integrity of the presently explored self-sourced reservoir (Macasty Formation) and its behaviour during hydraulic fracturing.

ACKNOWLEDGMENTS: Nancy Denommee (Parks Canada) is acknowledged for her help in providing access to Mingan islands. The authors thank Sébastien Castonguay and Stephan Séjourné for their review of the manuscript.

REFERENCES

Bai, T., Pollard, D.D., 2000. Fracture spacing in layered rocks : a new explanation based on the stress transition. Journal of Structural Geology, 22, 43-57.

Bai, T., Maerten, L., Gross, M.R., Aydin, A., 2002. Orthogonal cross joints: do they imply a regional stress rotation? Journal of Structural Geology, 24, 77-88.

Billi, A., Salvini, F., 2003. Development of systematic joints in response to flexure-related fibre stress in flexed foreland plates: the Apulian forebulge case history, Italy. Journal of Geodynamics, 36, 523-536.

Billi, A., Porreca, M., Faccenna, C., Mattei, M., 2006. Magnetic and structural constraints for the noncylindrical

evolution of a continental forebulge (Hyblea, Italy). Tectonics, 25, TC3011.

Bonnet, E., Bour, O., Odling, N.E., Davy, P., Main, I., Cowie, P., Berkowitz, B., 2001. Scaling of fracture systems in geological media. Reviews of Geophysics, 39, 347-383.

Bordet, E., Malo, M., Kirkwood, D., 2010. A structural study of western Anticosti Island, St. Lawrence platform, Quebec: A fracture analysis that integrates surface and subsurface structural data. Bulletin of the Canadian Petroleum Geology, 58, 36-55.

Caputo, R., 1995. Evolution of orthogonal sets of coeval extension joints. Terra Nova, 7, 479-490.

Castonguay, S., Wilson, R.A., Brisebois, D., Desrochers, A., Malo, M., 2005. Compilation géologique, Anticosti-Gaspé-Campbellton, les ponts géologiques de l'est du Canada, Transect 4, Québec-Nouveau-Brunswick. Commission Géologique du Canada, Open File 4883, 1:125 000, 4 sheets.

Cooper, M., Weissenberger, J., Knight, I., Hostad, D., Gillepsie, D., Williams, H., Burden, E., Porter-Chaudhry, J., Rae, D., Clark, E., 2001. Basin evolution in western Newfoundland: New insights from hydrocarbon exploration. American Association of Petroleum Geologists Bulletin, 85, 393-418.

Desrochers, A., 1988. Stratigraphie de l'Ordovicien de la région de l'Archipel de Mingan. Ministère des Ressources Naturelles du Québec, MM 87-01, 62p.

Desrochers, A., 2006. Rocky shoreline deposits in the lower Silurian (upper Llandovery, Telychian) Chicotte Formation, Anticosti Island, Quebec. Canadian Journal of Earth Sciences, 43, 1-10.

Desrochers, A., James, N.P., 1988. Early Paleozoic surface and subsurface paleokarst : Middle Ordovician Carbonates, Mingan Islands, Quebec. in: James, N.P., Choquette, P.W. (Eds), Paleokarst. Springer, London, pp. 183-210.

Desrochers, A., Brennan-Alpert, P., Lavoie, D. and Chi, G., 2012. Regional stratigraphic, depositional and diagenetic patterns from the interior of the St. Lawrence Platform: the Lower Ordovician Romaine Formation, western Anticosti Basin, Québec, in Derby, J R, Fritz, R D, Longacre, S A, Morgan, W A , Sternbach, C A. The great American carbonate bank: The geology and economic resources of the Cambrian - Ordovician Sauk megasequence of Laurentia, Memoir of the American Association of Petroleum Geologists, 98, pp.525-543.

Engelder, T., 1985. Loading paths to joint propagation during a tectonic cycle: an example from the Appalachian Plateau, U.S.A. Journal of Structural Geology, 7, 449-476.

Environnement Canada, 1991. Réserve de parc national de l'Archipel de Mingan: etude géologique et géomorphologique. Report by Entraco dated April 1991.

Ferrill, D.A., Morris, A.P., Hennings, P.H., Haddad, D.E, 2014. Faulting and fracturing in shale and self-sourced reservoirs: Introduction. American Association of Petroleum Geologists. 98, 2161-2164.

Lash, G.G., Engelder, T., 2007. Jointing within the outer arc of a forebulge at the onset of the Alleghanian Orogeny. Journal of Structural Geology, 29, 774-786.

Globensky, Y., 1987. Géologie des Basses-Terres du Saint-Laurent, Québec. Ministères des Richesses Naturelles, Québec, MM 85-02, 63 p.

Granier, T., Bles, , J.L., 1988. Déviation des contraintes et fractures de second ordre, région de Navacelles (Cause du Larzac, Massif Central français). Rapport Bureau de Recherche Géologique et Minière.

Hancock, P.L., Al Kadhi, A., Barka, A.A., Bevan, T.G., 1987. Aspects of anylising brittle structures. Annales tectonicae, 1, 5-19.

Long, D.G.F., 2007. Tempestite frequency curves: a key to Late Ordovician and Early Silurian subsidence, sea-level change and orbital forcing in the Anticosti foreland basin, Quebec, Canada. Canadian Journal of Earth Sciences, 44, 413-431.

Lynch, G., 2000. Shell Canada – Encal Energy, Anticosti Island Exploration 1997-2000. Ministère des Ressources Naturelles et de la Faune du Québec, Report 2000TD456-01, 32 p.

Mossop, G.D., Wallace-Dudley, K.E., Smith, G.G., Harrison, J.C., 2004. Sedimentary basins of Canada, Geological Survey of Canada, Open File 4673, 1 sheet.

Narr, W., Suppe, J., 1991. Joint spacing in sedimentary rocks. Journal of Structural Geology, 9, 1037-1048.

Nickelsen, R.P., Hough, V.N.D., 1967. Jointing in the Appalachian Plateau of Pennsylvania. Geological Society of America Bulletin, 78, 609-630.

Olson, J., Pollard, D.D., 1989. Inferring paleostresses from natural fracture patterns: a new method. Geology, 17, 345-348.

Pinet, N., Keating, P., Lavoie, L., Dietrich, J., Duchesne, M., Brake, V., 2012. Revisiting the Appalachian structural front and offshore Anticosti Basin (northern Gulf of St. Lawrence, Canada) by integrating old and new geophysical datasets. Marine and Petroleum Geology, 32, 50-62.

Reiter, K., Heidbach, O., Schmitt, D., Haug, K., Ziegler, M., Moeck, I., 2014. A revised crustal stress orientation database for Canada. Tectonophysics, 636, 111-124.

Rives, T., Rawnsley, K.D., Petit, J.P., 1994. Analogue simulation of natural orthogonal joint set formation in brittle varnish. Journal of Structural Geology, 16, 419-429.

Rustichelli, A., Agosta, F., Tondi, E., Spina, V., 2013. Spacing and distribution of bed-perpendicular joints throughout layered, shallow-marine carbonates (Granada Basin, southern Spain). Tectonophysics, 582, 188-204.

Sami, T., Desrochers, 1992. Episodic sedimentation on an early Silurian, storm-dominated carbonate ramp, Becscie and Merrimack formations, Anticosti Island, Canada. Sedimentology, 39, 355-381.

Sanford, B.V., 1993. St. Lawrence Platform-Geology, in: Scott, D.F., and Aitken, J.D. (Eds.), Sedimentary Cover of the Craton in Canada, Geological Survey of Canada, Geology of Canada, v. 5, pp. 723-786.

SOQUIP (Société Québecoise d'Initiatives Pétrolières), 1987. Estuary and Gulf St. Lawrence: Geological, Geophysical and Geochemical data integration. Geological Survey of Canada, Open File No 1721, 74 p.

Terzaghi, K., 1965. Source of error in joint surveys. Geotechnique, 15, 287-304.

Site No	Method	scan line strike	scan line length (m)	Number measurements	Formation	bed thickness
ANT-01	scan line - vertical wall	N2	17	40	Jupiter	0,08
ANT-02	scan line - vertical wall	N7	16	40	Jupiter	0,13
ANT-03	scan line - vertical wall	N135	40	41	Jupiter	0,4
ANT-05	scan line- vertical wall	N61	12	43	Jupiter	?
ANT-06	scan line - pavement	N112	45	2	Jupiter	0,4
ANT-07	scan line- vertical wall	N162	14.5	40	Jupiter	0,15
ANT-08	scan line- vertical wall	N40	12	20	Becsie	0,25
ANT-09	area sampling				Becsie	0,15
ANT-10	scan line - pavement	N27	8.5	40	Jupiter	0.08
ANT-12	scan line - vertical wall	N12	10	40	Jupiter	0.08
ANT-13	scan line - pavement	N70	9.5	40	Jupiter	0.1
ANT-14	scan line - pavement	N90	28.3	22	Chicotte	0.4
ANT-15	scan line - pavement	N42	58	25	Chicotte	0.2
ANT-16	circular scan line		63	12	Ellis Bay	?
ANT-17	scan line - pavement	N83	38.8	24	Vaureal	0.1
ANT-18	area sampling				Vaureal	0.15

Table 1a: Site characteristics - Anticosti Island

Site No	Method	scan line strike	scan line length (m)	Number measurements	Formation	bed thickness
MIN-01	scan line pavement circular scan line	N10 and N95	45 (N10) and 50 (N95) 88	49 (N10) and 23 (N95) 44	Mingan Mingan	0.6
MIN-02	circular scan line		94	52	Mingan	0.8
MIN-03	circular scan line		75	82	Mingan	0.4
MIN-04	circular scan line		94	41	Mingan	0.4
MIN-05	scan line - pavement circular scan line	N12 and N98	30 (N12) and 35 (N98) 94	16 (N12) and 16 (N98) 41	Mingan Mingan	0.2
MIN-06	circular scan line		94	26	Mingan	
MIN-07	scan line- vertical wall	N118	16	48	Romaine	0.6
MIN-08	scan line - vertical wall	N0 and N116	20 (N0) and 21 (N116)	25 (N0) and 34 (N116)	Romaine	0.2
MIN-09	scan line - pavement circular scan line	N97 and N03	61 (N97) and 31 (N03) 94	20 (N97) and 27 (N03) 52	Mingan	0.2
MIN-10	circular scan line		94	32	Mingan	0.4
MIN-11	circular scan line		94	30	Mingan	0.1
MIN-12	circular scan line		94	57	Mingan	0.4
MIN-13	scan line - pavement	96	31	45	Romaine	0.45
MIN-14	scan line- vertical wall	N54	28	46	Romaine	0.6

Table 1b: Site characteristics - Havre-Saint-Pierre/Mingan area

Site No	Most continuous set	Most frequent set	secondary set	fracture density measured - total	fracture density corrected - total	true spacing main set (+/- 10°)	Percent main and secondary sets	max length without fracture (measured)	comments
ANT-01	N105	N22	N105 or N22	2.4	4.3	1.2 (N105)	85	1.4	distinction between the main and secondary sets is not well constrained
ANT-02	N105	N15 +/-10	N15+/-10	2.5	4.3	1.1 (N105)	55	1.1	N160-N30 fractures may be overestimated due to trigonometric correction
ANT-03	N105	N105	N15	1.0	1.7	1.1 (N105)	83	4.9	vertical extent of fractures controlled by some (not all) lithological contact
ANT-05	N25 or N115	N25	N115	3.6	6.0	0.3 (N25)	79	1.3	main set characterized by fracture corridor with up to 5 fractures in 0.5 m. Secondary set often abuts against the main set
ANT-06	N110	N110	none	0,04		unknown		> 20	the scan line is parallel to the main fracture set
ANT-07	N115	N115	none	2.8	4.4	0.3 (N115)	75	1.2	fracture corridor with up to 7 fractures in 0.65 m
ANT-08	none	N105	N20	1.7	2.6	1.1 (N105)	67	1.9	maximal fracture length = 1m
ANT-09	N95	N120		1.7	1.7	around 3		2.2	the main set exhibits a complex geometry; bedding not well defined
ANT-10	N100	N10?	N10 and N75	4.7	8.3	0.9	45	0.5	the main set is longer, more planar and other sets abut against it. Trigonometric correction may have led to an overestimation of secondary sets
ANT-12	N97	N97	N10	4	5.6	0.3	77	0.6	fracture corridor. Fractures parallel to the scanlie may be underestimated. 2 fractures with dip less than 80°
ANT-13	N97	N97	N10	4.2	9.5	0.2	83	0.7	rectangular blocks with quite constant elongation (length = 3 width)
ANT-14	N15	N15	?	0.8	0.9	2.0	64	3.4	fractures parallel to the scanline may be underestimated
ANT-15	poorly defined N85 +/- 20	poorly defined N85 +/- 20	?	0.4	0.8	3.2 (N85)	40	10	Most fractures have 2 end points (no abutting relationship)
ANT-16	N110	110	?	0.2	0.2				very few fracture. Irregular bedding surface
ANT-17	N100	N100	N10	0.6	1.5	0.8	98	10.1	
ANT-18	N98	N98	N20						en échelon fracture

Table 2a: Main joint characteristics - Anticosti Island

Site No	Most continuous set	Most frequent set	secondary set	fracture density measured - total	fracture density corrected - total	true spacing main set (+/- 10°)	Percent main and secondary sets	max length without frature (measured)	comments
MIN-01	N95	N95	N10	0,8 0.5	0.8 0.5	0.9	86	5.2	field data indicate that the N10 set predomintly abuts againt the N95 set. Photo of the outcrop suggests an opposite result
MIN-02	N80			0.6	0.6				
MIN-03				1.1	1.1				en échelon fracture suggesting some left-lateral motion.
MIN-04	N96			0.4	0.4				
MIN-05	N95	N95	N10	0.5 0.4	0.5 0.4	1.9	76	4.2	the main set is longuer; secondary set abuts more frequently against the main set
MIN-06	N16			0.3	0.3				
MIN-07	N15 or N105	N15 or N105	N15 or N105	3	4.5	0.5 (N15) - 0.4 (N105)	98	0.9	two fracture planes exhibit evidence of sinistral motion (slickenline)
MIN-08	N95	N95	N5	1.4	2.2	1.2	59	5.3	N95 set is the more continuous
MIN-09	N10 ?	N95	N95 ?	0.6 0.6	0.6 0.6	3.0 (N10)	73	14.8	
MIN-10	N98			0.3	0.3				
MIN-11	?			0.3	0.3				irregular fracture pattern
MIN-12				0.6	0.6				rectangular pattern
MIN-13	N100	N10	N10?	1.5	?	? 0.9 (N10)	high	3.2 (N10)	impossibility to quantify the N100 set
MIN-14	N15	N15	N115	1.6	2.5	0.8	70	2.7	

Table 2b: Main joint characteristics - Havre-Saint-Pierre/Mingan area